

# On the development of a ship simulation model for maneuvering tasks in waves

Maria ACANFORA<sup>a,1</sup> Marco ALTOSOLE<sup>a</sup>, Ernesto FASANO<sup>a</sup>, and Davide LAURIA<sup>a</sup>

<sup>a</sup>*University of Naples "Federico II", Department of Industrial Engineering, Italy*

**Abstract.** The possibility of simulating the interaction of hull, propeller, and engine is gathering the interest of several researches, in view of a more realistic design and control of the whole propulsion chain. The engine performance in rough seas is affected by the dynamics of the hull and consequently by the complex flow regime at the propeller, which induces fluctuating engine torques and revolutions. In a previous research, the case study was limited to straight run simulations in irregular waves for a Ro-pax ferry, including the power delivery contribution by a diesel engine. Herein, the numerical simulation model is further developed for allowing the simulation of the main engine behavior in waves during maneuvering tasks. In order to assess the accuracy and the limits of applicability of the implemented maneuvering model, a benchmark ship is introduced, i.e. the KVLCC2, for which several experimental data are available in the technical literature. The focus on the numerical modeling for the KVLCC2 stays in the implementation of a comprehensive maneuvering model (i.e. including rudder and propeller interactions), capable of simulating the complex dynamics of a ship maneuvering in waves with a fair level of accuracy. The comparisons between simulation and experimental data will disclose the range of applicability and the validity of the numerical models under investigation.

**Keywords.** Ship dynamics, numerical simulation, maneuvering

## 1. Introduction

The IMO has set ambitious decarbonisation targets for the marine industry, bringing the attentions of ship owners towards alternative propulsion systems. In [1], a wide description of all possible combinations of hybrid propulsion systems was provided. Several considerations on practical applications in the maritime sector are available in the more recent technical literature: for example, in [2], [3] the authors studied the feasibility of adopting fuel cell on board ships; in [4] the authors focused on battery-powered vessels for zero-emission purposes. In this context, the possibility to simulate beforehand the performances of these hybrid propulsion systems on board ships represents a valuable contribution in terms of design and control [5]. Therefore, this sets the need for a comprehensive numerical simulator of ship dynamics and ship propulsion chain. A good simulator of marine propulsion systems is made up of several numerical sub-models that reproduce the main elements involved in ship propulsion chain. Among these sub-models, the prime mover strongly characterizes the complexity of the simulator. It is known that engine performance in rough seas is affected by the dynamics of the hull and consequently by the complex flow regime at

---

<sup>1</sup> Corresponding Author, Maria Acanfora, Department of Industrial Engineering, University of Naples "Federico II", Napoli, Via Claudio 21, Italy; E-mail: maria.acanfora@unina.it.

the propeller, which induces fluctuating engine torques and revolutions [6], [7]; therefore sub-models for ship dynamics, and propeller characteristics are deemed necessary. Moreover, ship maneuvers also affects propulsion system performances due to the changes of speed and sailing direction that have direct implications for propeller behavior and thus for the propulsion system.

In (Acanfora et al. 2021), a numerical simulation model, accounting for hull propeller engine interactions was developed. The numerical model for hull dynamics in irregular waves was validated in [8]; the numerical engine model was finely developed and calibrated in [9]; and the numerical model for propeller characteristics was developed in [6] based on experimental evidences. Among the current sub-models, the maneuvering numerical model is still under development in the simulator. In [10], a linear maneuvering model was implemented and the flow interaction between rudder and propeller was disregarded: the obtained outcomes, regarding turning circle in irregular waves at constant speed, were found satisfying for the Ro-pax ship under investigation. Nevertheless, this approach cannot be generalized. In particular, it was concluded that in case of a constant speed condition it might be possible neglecting rudder-propeller interaction without inducing large errors, whereas this is not doable in case of a constant revolution conditions. The numerical model for maneuvering in still water is generally non-linear, depending on the hull form, and it is based on the knowledge of the so-called maneuvering coefficients. This approach is well consolidated in the technical literature [11] and it is completed by the rudder model. The effects of hull and propeller on the rudder can be modeled following different approaches: one available in [12] is based on analytical hydrodynamic considerations; the other one, that goes under the name of MMG method [13] is based on the knowledge of numerical coefficients available from experimental test, or from numerical CFD analysis [14]. The main issue, when dealing with maneuvering in wave simulations, stays in the coexistence of high frequency dynamics (due to waves) and low frequency dynamics (due to maneuvers). Indeed, several techniques were developed to solve this problem such as: the convolution integral technique [15]; the so-called two-time scale approach [16]; and the direct superposition of maneuvering and sea-keeping model [12], [17].

In this paper, we implement the MMG approach for rudder and maneuvering models together with the direct superposition approach in waves. The hull chosen for the applications is the so called KVLCC2, for which all experimental input data are available [13], in addition to the experimental tests of turning circle in regular waves for validation purposes [18]. The overall comparisons between simulation outcomes and experimental data will help in assessing the pros and cons of the applied methods in view of future applications concerning hull-rudder-propeller-engine interactions during maneuvering tasks. Following, a modified version of the direct superposition technique will be proposed and applied, in view of further improvements of the current simulation model.

## **2. Numerical model for the hull dynamics in waves**

The non-linear 6DOF model for hull dynamics in regular and irregular waves is based on the equations of motions for a rigid ship (see (1)) of mass  $m$ .

The numerical model can be defined as hybrid or blended, and it is based on the assumptions explained in [12], where additional details and information on the

reference frames are available. In particular, the equation (1) is expressed in the body fixed reference frame centered at the ship center of gravity.

$$\begin{cases} (m + a_{11})\dot{u} + m(qw - rv) + a_{15}\dot{q} = -mgsin\theta + X_{wave} + X_{man} - k_{11} - k_{15} + X_{prop} + X_{res} + X_{rud} \\ (m + a_{22})\dot{v} + m(ru - pw) + a_{24}\dot{p} + a_{26}\dot{r} = mgcos\theta sin\phi + Y_{wave} + Y_{man} - k_{22} - k_{24} - k_{26} + Y_{rud} \\ (m + a_{33})\dot{w} + m(pv - qu) + a_{35}\dot{q} = mgcos\theta cos\phi + Z_{wave} - k_{33} - k_{35} \\ (I_x + a_{44})\dot{p} + (I_z - I_y)qr + a_{42}\dot{v} + a_{46}\dot{r} = K_{wave} + K_{man} - k_{44} - k_{42} - k_{46} + K_{rud} \\ (I_y + a_{55})\dot{q} + (I_x - I_z)rp + a_{15}\dot{u} + a_{53}\dot{w} = M_{wave} - k_{55} - k_{53} - k_{31} \\ (I_z + a_{66})\dot{r} + (I_y - I_x)pq + a_{62}\dot{v} + a_{64}\dot{p} = N_{wave} + N_{man} - k_{66} - k_{62} - k_{64} + N_{rud} \end{cases} \quad (1)$$

The terms  $a_{ij}$  and  $k_{ij}$  (with  $i$  and  $j$  from 1 to 6) are, respectively, the added mass coefficients corresponding to the infinite frequency, and elements of the memory function [19], modelling radiation actions in irregular sea. In modelling irregular sea damping, viscous components are disregarded. The terms with the subscript “wave” include Froude-Krylov, diffraction and restoring forces and moments, as explained in [8], [12]. The terms with the subscript “man” refer to manoeuvring actions, the terms with the subscript “prop” and “resist” refer to propeller and resistance forces, while the term with the subscript “rud” refer to rudder actions. Additional details for these forces and moments are provided in the following sections. The inertia, Froude-Krylov and restoring forces and moments are evaluated accounting for all the relevant nonlinearities. The pressure profile is assumed by applying the so-called “stretched distribution” above the waterline. This approach is a kind of extension of the linear wave theory to incorporate the nonlinear effects associated with the variation of the free surface. The hull is discretized by means of triangular panel.

### 2.1. Non-linear model of maneuvering actions in waves

The non-linear model of manoeuvring in waves takes into account the non-linear manoeuvring coefficients in still water, coming from the series expansion of the fluid force. Applying the symmetry assumption of [20] and limiting the manoeuvring derivatives to the more relevant terms, the non-linear manoeuvring forces in body fixed axis, can be expressed as follows:

$$\begin{cases} X_{man} = X_{vv}v^2 + X_{rr}r^2 + X_{vr}vr + X_{vvvv}v^4 \\ Y_{man} = Y_vv + Y_r r + Y_{vvv}v^3 + Y_{rrr}r^3 + Y_{rrv}vr^2 + Y_{vvr}rv^2 \\ N_{man} = N_vv + N_r r + N_{vvv}v^3 + N_{rrr}r^3 + N_{rrv}vr^2 + N_{vvr}rv^2 \\ K_{man} = -Y_{man}(Z_G - T/2) \end{cases} \quad (2)$$

Based on the direct superposition approach for maneuvers in waves, the derivatives related to the accelerations, that are usually an essential part of the still water models for ship maneuvers, herein are disregarded, since their effects are already included into the added mass terms  $a_{ij}$ . On the other hand, the potential damping terms  $k_{ij}$  of ship dynamics in waves, in the sway and yaw directions (i.e.,  $i$  and  $j$  equal to 2 and 6), are disregarded when the maneuvering model is superposed to the seakeeping model. In this way, the maneuvering derivatives are multiplied by the sway and yaw velocities ( $v$  and  $r$  respectively) that are characterized by high and low frequency components, due to seakeeping and maneuvering dynamics respectively.

Although direct superposition approach proved to be fairly accurate for modeling such complex dynamics [11], [12], there are still margins for improvements. The current development in the direct superposition method bases on the decomposition of sway and yaw velocities into high frequency signal ( $v^+$  and  $r^+$ ) and low frequency signal ( $v^-$  and  $r^-$ ). This allows for force decomposition: maneuvering forces are obtained by multiplying maneuvering derivatives for  $v^-$  and  $r^-$  while by seakeeping forces are obtained using  $v^+$  and  $r^+$  for the evaluation of the damping terms  $k_{ij}$  ( $i$  and  $j$  equal to 2 and 6). This approach would combine the characteristics of the unified maneuvering models with the characteristics of the two-time scale models.

In this paper, we propose a filtering technique based on an exponential filter, as described in section 3, aiming at minimizing the signal delay, for sway and yaw velocity decomposition.

## 2.2. Numerical model of ship resistance and propulsion in waves

In the current simulation model, ship resistance in still water is given by (3). Added wave resistance accounts for first order effects and it includes restoring and Froude-Krylov non-linear (components evaluated on the tridimensional panel discretization of the hull) together an approximate estimation of radiation and diffraction forces from linear strip-theory approach [21].

$$X_{res} = \frac{1}{2} \rho V_S^2 S C_T \quad (3)$$

Therefore, the range of applicability of this numerical model for ship resistance in waves reasonably limits to the sea states characterized by wave length greater than ship length, where radiation and diffraction actions are not predominant.

The numerical model of the sailing ship in waves includes screw propeller actions that are implemented by means of still water propeller coefficient  $K_T$  and  $K_Q$ , given as function of the advance coefficient  $J$ . The thrust  $T_{prop}$  and the torque  $Q_{prop}$  at the propeller are:

$$T_{prop} = \rho K_T N_{prop}^2 D_{prop}^4 \quad Q_{prop} = \rho K_Q N_{prop}^2 D_{prop}^5 \quad (4)$$

Differently from [22], propeller thrust and torque are obtained without applying any correction due to propeller emersion. In (5) the thrust deduction factor refers to the still water condition also for wave simulations.

$$X_{prop} = (1 - t_p) T_{prop} \quad (5)$$

## 2.3. The MMG model for steering actions

The so-called MMG standard model is one of the solutions for ship manoeuvring simulations in still water [23] developed by the Japanese Manoeuvring Modelling research Group from which the MMG name derives [13], [24]. In this paper, we focus on the peculiar modeling of the hydrodynamic forces exerted by the rudder (6), provided by the MMG method. The method bases on the knowledge of pertinent experimental coefficients for the estimation of steering actions, in order to account for the evidence that rudder operates in the slipstream induced by hull and propeller.

$$\begin{cases} X_{RUD} = -(1 - t_r) F_N \sin \delta \\ Y_{RUD} = (1 + a_h) F_N \cos \delta \\ K_{RUD} = -(1 + a_h) Z_{rud} F_N \cos \delta \\ N_{RUD} = (X_{rud} + a_h x_h) F_N \cos \delta \end{cases} \quad (6)$$

$F_N$  is the rudder normal force (see (7)),  $t_r$ ,  $a_h$  and  $x_h$  are the coefficients representing the hydrodynamic interaction between hull and rudder. In particular,  $t_r$ , called the steering resistance deduction factor, includes also for propeller effects of the rudder.

Rudder normal force  $F_N$  is expressed as:

$$F_N = \frac{1}{2} \rho A_R U_R^2 f_\alpha \sin \alpha_R \quad (7)$$

where  $A_R$  is the rudded area,  $f_\alpha$  is the rudder lift coefficient,  $U_R$  is the resultant inflow velocity and  $\alpha_R$  is the inflow angle, defined as follows:

$$U_R = \sqrt{u_R^2 + v_R^2} \quad (8)$$

$$\alpha_R = \delta - \tan^{-1}\left(\frac{v_R}{u_R}\right) \simeq \delta - \frac{v_R}{u_R} \quad (9)$$

In (9),  $\delta$  is the rudder deflection angle,  $u_R$  and  $v_R$  are the longitudinal and lateral inflow velocity components to rudder, respectively, that account for hull dynamics and propeller effects. In particular, longitudinal inflow depends on rudder and propeller interactions, while lateral inflow accounts for flow straightening effects modeled by the so-called flow-straightening coefficient. Additional details and formulas, herein omitted for the sake of synthesis, are available in [13].

#### 2.4. Developed filtering technique

The filtering technique is based on the so-called exponential smoothing approach, where the smoothing coefficient is  $\alpha_s = dt/\tau$ . The sample time  $dt$  is herein assumed as  $dt=0.3$  s, while  $\tau$  represents the encounter period of the ship, that modifies during the simulation. In the current model, a second order transfer function is adopted, in order to minimize the phase shift that the exponential smoothing technique would induce in the filtered signal.

### 3. Case study

The KVLCC2 is a very large crude carrier developed by the KRISO towing tank for research purposes and used for several benchmark studies [18], [25].

**Table 1.** Main characteristics of KVLCC2

Characteristic	Value
Length between perpendiculars, L [m]	320
Breadth, B [m]	58
Draft, T [m]	20.8
Displacement [m <sup>3</sup> ]	312622
Long. center of gravity LCG from aft perp. [m]	171.1
Vertical center of gravity VCG [m]	18.56
Roll radius of gyration [B]	0.4
Yaw radius of gyration [L]	0.25
Rudder lateral area [m <sup>2</sup> ]	136.7
Turn rate [degree/s]	2.34
Propeller Diameter [m]	9.86

The hull data, in ship scale, are given in table 1.

The main manoeuvring derivatives and the hydrodynamic coefficients used for the implementation of manoeuvring and steering models are taken from [11], [13].

The case study concerns the numerical simulation of turning circle manoeuvres in regular waves for two wavelengths ( $\lambda/L=1$  and  $\lambda/L=1.5$ ), two wave directions ( $\beta=180^\circ$  and  $\beta=270^\circ$ , with  $\beta=180^\circ$  head sea) and three wave height ( $H/L=0.02$ ,  $H/L=0.015$ , and  $H/L=0.01$ ). The obtained outcomes, in terms of turning circle path, are qualitatively compared with the experimental data available in [18].

#### 4. Results

Prior to show the results referring to turning circle in waves, a preliminary analysis in still water is carried out. The comparison between the experimental data and the numerical simulation (see Fig. 1) confirms that the implemented maneuvering model with the MMG approach provides an accurate modeling of the turning path in still water. In this section, we mainly focus on the applications of the direct superposition method, i.e. without filtering and decomposing sway and yaw velocities. Figure 1 shows the turning circle paths for a wavelength equal to ship length ( $\lambda/L=1$ ) and two different initial encounter angles  $\beta$ . The comparison with the experimental data is carried out by superposition of the numerical data on the graphical experimental result. The turning circle in head wave  $\beta=180^\circ$  shows a drifting direction rearward and leftward; whereas the turning circle in beam waves coming from the left side of the hull  $\beta=270^\circ$  shows a drifting direction mainly rightward and leftward. Despite the experimental and the numerical trajectories are not perfectly matching, the drifting directions are properly simulated. In Fig. 2, the comparison between experimental and numerical data, is shown for three different wave height, for the turning circle in head waves to portside,  $\lambda/L=1$ , given the availability of experimental graphical results from [18]. Figures 2a, 2b and 2c refer to  $H/L=0.02$ ,  $H/L=0.015$ , and  $H/L=0.01$  respectively. It is possible noticing that the larger is the wave height the greater is the drifting distance. This trend, together with the drifting direction (rearward and rightward) is fairly simulated. Moreover, for the smaller wave height  $H/L=0.01$ , the numerical turning circle path resembles the experimental data with a good accuracy.

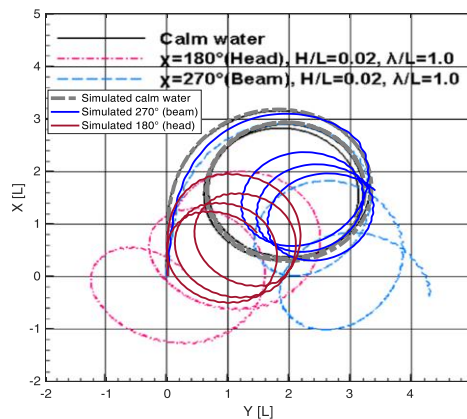
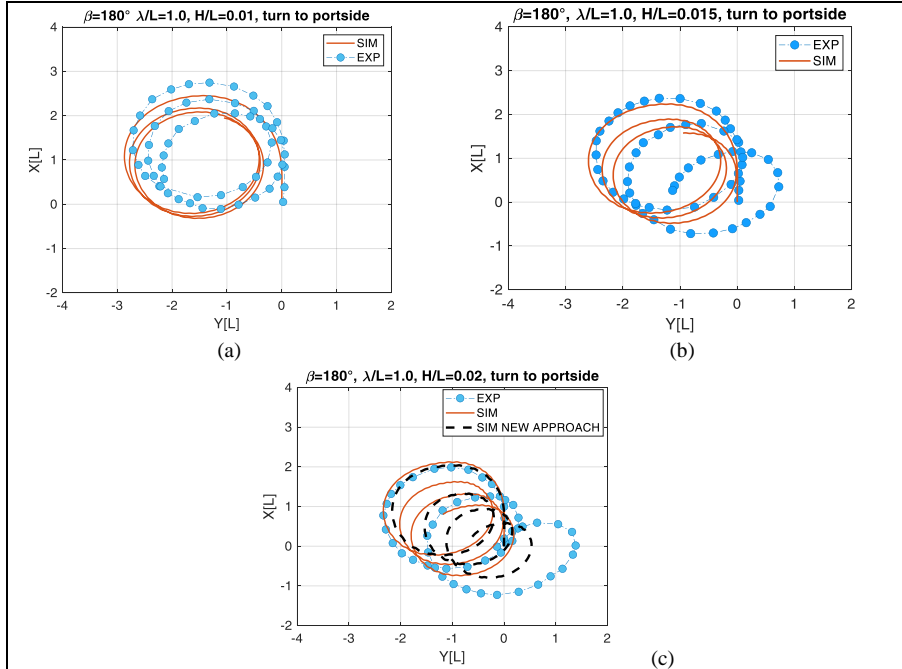


Figure 1. turning circle in head and beam waves to starboardside,  $\delta=-35^\circ$ .



**Figure 2.** turning circle in head waves  $\lambda/L=1$  , to portside,  $\delta=35^\circ$  for different wave heights

In Fig. 3, the comparison between experimental and numerical data is shown for  $\lambda/L=1.5$  and  $H/L=0.02$  in case of beam and head waves. The obtained numerical outcomes confirm a qualitative good accuracy with the experimental measurements, especially for  $\beta=270^\circ$ .

From the analysed results, it seems that the overall agreement of the numerical model improves noticeably by increasing the wavelength and reducing the wave amplitude in case of shorter waves. Nevertheless, the presented outcomes are in the same range of accuracy of other models dealing with the numerical simulation of turning circle in regular waves [25], [26].

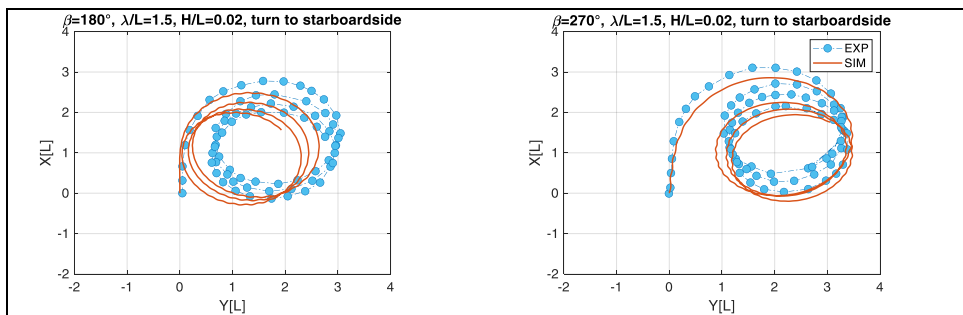


**Figure 3.** turning circle in head waves  $\lambda/L=1.5$  , to starboard,  $\delta=35^\circ$  for different encounter angles

The application of the novel approach, including the decomposition of the sway and yaw velocities, is carried out for wavelength condition  $\lambda/L=1$ ,  $H/L=0.02$  in head wave. The fair accuracy of the filter can be observed in Fig. 4 for the sway velocity: the current approach minimize the signal delay, although it is not fully efficient in the

smoothing action. The obtained turning circle path is shown in Fig. 2c, aiming at comparing the new simulation approach with the experimental data and with the outcomes of the unchanged simulation model. It is possible noticing how the new approach has a certain improvement in modelling the initial part of the turning circle and has a better agreement in the drifting distances, in spite of somewhat smaller turning diameters compared to the unchanged simulation model outcomes. Indeed, such differences in turning diameters and in drifting distances are responsible for almost an additional simulated turn compared to the experimental data.

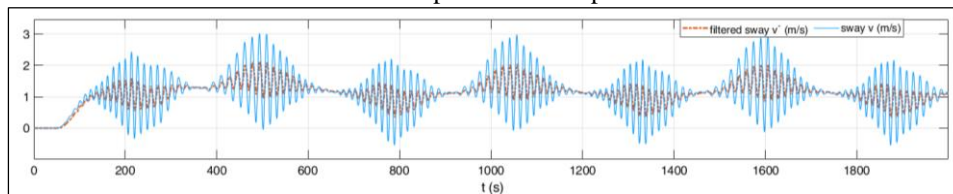


**Figure 4.** Filtered sway velocity during turning circle in head waves,  $\lambda/L=1$ , to portside,  $H/L=0.02$

## 5. Conclusions

In this paper, we presented a numerical model for ship manoeuvring in waves applied to a large tanker for the estimation of the turning circle paths. The comparison with the experimental data confirmed a fair accuracy of the model for increasing wavelengths. Nevertheless, an overall agreement in the drifting directions due to the different wave conditions under investigation was always appreciable. Although there are several acknowledged limitations in the numerical model, the obtained results fall within the same range of accuracy of similar researches. In addition, the developed approach, based on signal decomposition by means of exponential smoothing, proved to have a certain improvement for the turning circle case where it was applied. Therefore, future studies will focus on the refinement of such technique with additional applications.

## References

- [1] O. B. Inal, J.-F. Charpentier, and C. Deniz, "Hybrid power and propulsion systems for ships: Current status and future challenges," *Renew. Sustain. Energy Rev.*, vol. 156, 2022.
- [2] L. Micoli, T. Coppola, and M. Turco, "A Case Study of a Solid Oxide Fuel Cell Plant on Board a Cruise Ship," *J. Mar. Sci. Appl.*, vol. 20, no. 3, pp. 524–533, 2021.
- [3] M. Perčić, N. Vladimir, I. Jovanović, and M. Koričan, "Application of fuel cells with zero-carbon fuels in short-sea shipping," *Appl. Energy*, vol. 309, 2022.
- [4] H. Wang, E. Boulougouris, G. Theotokatos, P. Zhou, A. Priftis, and G. Shi, "Life cycle analysis and cost assessment of a battery powered ferry," *Ocean Eng.*, vol. 241, 2021.
- [5] S. Saettone *et al.*, "The importance of the engine-propeller model accuracy on the performance prediction of a marine propulsion system in the presence of waves," *Appl. Ocean Res.*, vol. 103, p. 102320, Oct. 2020.
- [6] O. N. Smogeli, "Control of Marine Propellers from Normal to Extreme Conditions," Faculty of Engineering Science & Technology, 2006.
- [7] M. H. Ghaemi and H. Zeraatgar, "Analysis of hull, propeller and engine interactions in regular waves by a combination of experiment and simulation," vol. 26, pp. 257–272, 2021.
- [8] M. Acanfora and E. Rizzuto, "Time domain predictions of inertial loads on a drifting ship in irregular beam waves," *Ocean Eng.*, vol. 174, pp. 135–147, Feb. 2019.
- [9] G. Benvenuto, U. Campora, M. Laviola, and G. Terlizzi, "Simulation model of a dual-fuel four stroke engine for low emission ship propulsion applications," *Int. Rev. Mech. Eng.*, vol. 11, no. 11,



pp. 817–824, 2017.

- [10] M. Acanfora and F. Balsamo, “The Smart Detection of Ship Severe Roll Motions and Decision-Making for Evasive Actions,” *J. Mar. Sci. Eng.*, vol. 8, no. 6, p. 415, Jun. 2020.
- [11] G. Taimuri, J. Matusiak, T. Mikkola, P. Kujala, and S. Hirdaris, “A 6-DoF maneuvering model for the rapid estimation of hydrodynamic actions in deep and shallow waters,” *Ocean Eng.*, vol. 218, p. 108103, 2020.
- [12] J. Matusiak, *Dynamics of a Rigid Ship -with applications*. Aalto University publication series SCIENCE + TECHNOLOGY, 4/2021, 2021.
- [13] H. Yasukawa and Y. Yoshimura, “Introduction of MMG standard method for ship maneuvering predictions,” *J. Mar. Sci. Technol.*, vol. 20, no. 1, pp. 37–52, 2015.
- [14] D. Villa, A. Franceschi, and M. Viviani, “Numerical analysis of the rudder-propeller interaction,” *J. Mar. Sci. Eng.*, vol. 8, no. 12, pp. 1–22, 2020.
- [15] T. I. Fossen, “a Nonlinear Unified State-Space Model for Ship Maneuvering and Control in a Seaway,” *Int. J. Bifurc. Chaos*, vol. 15, no. 09, pp. 2717–2746, 2005.
- [16] R. Skejic and O. M. Faltinsen, “A unified seakeeping and maneuvering analysis of ships in regular waves,” *J. Mar. Sci. Technol.*, vol. 13, no. 123, pp. 371–394, 2008.
- [17] M. Acanfora and J. Matusiak, “On the estimations of ship motions during maneuvering tasks in irregular seas,” in *Proceedings of 3rd International Conference on Maritime Technology and Engineering, MARTECH 2016*, 2016, vol. 1.
- [18] D. J. Kim, K. Yun, J.-Y. Park, D. J. Yeo, and Y. G. Kim, “Experimental investigation on turning characteristics of KVLCC2 tanker in regular waves,” *Ocean Eng.*, vol. 175, pp. 197–206, Mar. 2019.
- [19] W. E. Cummins, “The impulse response function and ship motions,” 1962.
- [20] M. S. Triantafyllou and F. S. Hover, “Maneuvering and Control of Marine Vehicles,” *Maneuvering Control Mar. Veh.*, pp. 105–110, 2003.
- [21] T. Kukkanen and J. Matusiak, “Nonlinear hull girder loads of a RoPax ship,” *Ocean Eng.*, vol. 75, pp. 1–14, 2014.
- [22] M. Acanfora, M. Altosole, F. Balsamo, L. Micoli, and U. Campora, “Simulation Modeling of a Ship Propulsion System in Waves for Simulation Modeling of a Ship Propulsion System in Waves for Control Purposes,” 2022.
- [23] B. Piaggio, M. Viviani, M. Martelli, and M. Figari, “Z-Drive Escort Tug manoeuvrability model and simulation,” *Ocean Eng.*, vol. 191, 2019.
- [24] Y. Yoshimura, “Mathematical Model for Manoeuvring Ship Motion (MMG Model),” in *Workshop on Mathematical Models for Operations Involving Ship-Ship Interaction, Tokyo*, 2005, no. August, pp. 1–6.
- [25] V. Shigunov, O. el Moctar, A. Papanikolaou, R. Potthoff, and S. Liu, “International benchmark study on numerical simulation methods for prediction of manoeuvrability of ships in waves,” *Ocean Eng.*, vol. 165, pp. 365–385, Oct. 2018.
- [26] R. Suzuki, M. Ueno, and Y. Tsukada, “Numerical simulation of 6-degrees-of-freedom motions for a manoeuvring ship in regular waves,” *Appl. Ocean Res.*, vol. 113, p. 102732, Aug. 2021.